(Fig. 1). ACF were defined as lesions with larger crypts and showing darker staining with methylene blue than normal crypts, often with oval or slit-like lumens, and a thicker epithelial lining (Fig. 1).

Histological examination of the identified colonic mucosal lesions. After identification and measurement of the MDF and ACF, each lesion was dissected and embedded in paraffin for histological analysis. Each section was basically examined using an en face preparation, and, in addition, some lesions were also examined in longitudinal preparations. The 4-μm-thick sections were stained with H&E and evaluated by at least two pathologists. Immunohistochemical staining for MUC2 protein (Santa Cruz Biotechnology, Santa Cruz, CA, USA) was also performed on each of the serial HE-stained sections, using the universal immuno-enzyme polymer method with microwave activation (Simple Stain MAX PO M kit; Nichirei, Tokyo, Japan).

Results

Identification of aberrant crypt foci and mucin-depleted foci in the colon of sporadic colorectal cancer patients. Colonic samples were stained with AB, pH 2.5, to identify the presence of MDF, and subsequently stained with methylene blue to identify the presence of ACF. As expected, both ACF and MDF were easily visualized. MDF could be distinguished into two categories: flat-MDF and protruded-MDF (Fig. 1F and K, respectively). The characteristics of these colonic lesions are shown in Table 2. We found a total of 354, 41 and 19 colonic mucosal lesions with a mean multiplicity of 44, 38.9 and 66.9 crypts (ACF, flat-MDF and protruded-MDF, respectively). In this study, the density of MDF (flat-MDF and protruded-MDF) was 0.0082 lesions/cm^2, which is higher than that reported in sporadic CRC patients (0.0006 lesions/cm^2).[19] The multiplicity of crypts in the protruded-MDF was significantly higher than that in any of the other lesions ($P = 0.02$). In regard to the locations of these colonic lesions, the density of ACF was significantly higher in the left colon than that in the right colon ($P = 0.011$). This trend was similar to the epidemiology of CRC.[2] In contrast, the density of flat-MDF and protruded-MDF were higher in the left colon than in the right colon, although the differences were not statistically significant ($P = 0.063$ and $P = 0.61$, respectively).

Histological analysis of the identified aberrant crypt foci and mucin-depleted foci in the colons of sporadic colorectal cancer patients. The identified flat-MDF (41 lesions), protruded-MDF (19 lesions) and the representative sample of ACF (20 lesions) were sectioned for histopathology. Three different types of crypt foci were identified in the HE-stained sections. ACF were characterized by larger crypts and wider lumens, as compared with the surrounding crypts, corresponding to hyperplastic or non-dysplasic lesions (Fig. 1C–E). In contrast, the flat-MDF did not show nuclear stratification or loss of polarity, but showed Paneth cell metaplasia and decrease/loss of goblet cells, indicative of low-grade dysplasia (Fig. 1H–J). Protruded-MDF showed the features of both ACF and MDF, also corresponding to low-grade dysplasia (Fig. 1M–O). We also detected inflammatory cell infiltration as a specific histological feature of MDF (Fig. 1J,O). Immunohistochemical staining for MUC2 revealed that MDF were depleted of MUC2 expression, the most abundant type of mucin in the colon (Fig. 2).

Examination of mucin-depleted foci in the familial adenomatous polyposis patient. The density of MDF in the FAP patient was 0.068 lesions/cm^2, which was much higher than that in the sporadic CRC patients in this study, similar to Femia's report. All the MDF (eight lesions) from the FAP patient were flat-MDF, and showed slight nuclear stratification and loss of polarity, and Paneth cell metaplasia, corresponding to moderate-grade dysplasia (Fig. 3).

Table 2. Characteristics of the colonic mucosal lesions in colorectal cancer patients

	ACF	Flat-MDF	Protruded-MDF
Total number	354	41	19
Number/patient	6.7 ± 6.9	0.8 ± 1.5	0.4 ± 0.9
Crypts/lesion*	44.0 ± 55.7	38.9 ± 62.7	66.9 ± 82.6
Density (lesion/cm^2)†			
Total colon	0.054 ± 0.058	0.007 ± 0.017	0.003 ± 0.009
Right colon	0.023 ± 0.034	0.002 ± 0.006	0.001 ± 0.003
Left colon	0.067 ± 0.061	0.009 ± 0.019	0.004 ± 0.010

Right colon: ascending colon and transverse colon. Left colon: descending colon, sigmoid colon, and rectum. Values are mean ± SD. *$P = 0.02$ calculated by Kruskal–Wallis test. †The differences in the density of the colonic mucosal lesions between the right colon and left colon was calculated by the Mann–Whitney U-test ($P = 0.011$, $P = 0.063$ and $P = 0.61$, ACF, flat-MDF and protruded-MDF, respectively).

Discussion

Although previous published studies reveal that some ACF show dysplastic changes and might serve as surrogate biomarkers of colorectal carcinogenesis, the majority of ACF in CRC patients are not dysplastic.[11,22–27] Consistent with these reports, we confirmed that representative samples of ACF from sporadic CRC patients corresponded to hyperplastic or non-dysplastic lesions. In contrast, protruded-MDF, which have the characteristics of both ACF and MDF, showed changes corresponding to low-grade dysplasia. In addition, we revealed that protruded-MDF have a larger number of crypts than ACF. ACF with a large number of crypts have been reported to show a stronger correlation with the presence of CRC than those with a small number of crypts.[11] Thus, the results in the present study suggest that protruded-MDF might, at least in part, correspond to dysplastic ACF and probably represent more advanced lesions in colorectal carcinogenesis.

In our study, the density of MDF in sporadic CRC patients was much higher than that reported from a previous study.[19] We analyzed larger areas of the colorectum, which could partially explain our finding a higher number of MDF. However, this is not sufficient to explain the discrepancy; another reason might be differences in the characteristics of the study participants, such as race and age. For example, ACF are reported to be detected at a higher incidence in Japanese patients than in American patients.[11,14,27,28] Yet another reason might be the difference in the method of detection used between the two studies. MDF were originally identified using a stain for more stringent mucin staining; namely, high iron diamine-AB.[19] In experimental models, we previously showed that approximately one-quarter of the MDF identified with AB staining were actually normal-like crypts, and approximately 10% of MDF identified with AB staining corresponded to classical ACF with dysplasia.[21] MDF identified in the present study might contain these lesions, and this could explain the higher density of MDF in our study.

Concerning the histological characteristics of MDF, MDF identified in sporadic CRC patients showed changes corresponding to low-grade dysplasia. Paneth cell metaplasia, which has been shown to be correlated with the presence of CRC,[29] was also observed in both flat-MDF and protruded-MDF; however, no nuclear stratification or loss of polarity was observed. In contrast, MDF identified in the FAP patient showed slight nuclear stratification and loss of polarity, corresponding to moderate-grade dysplasia. Indeed, our sample size was too small to conclude the histopathological characteristics of MDF in FAP

doi: 10.1111/j.1349-7006.2011.02125.x

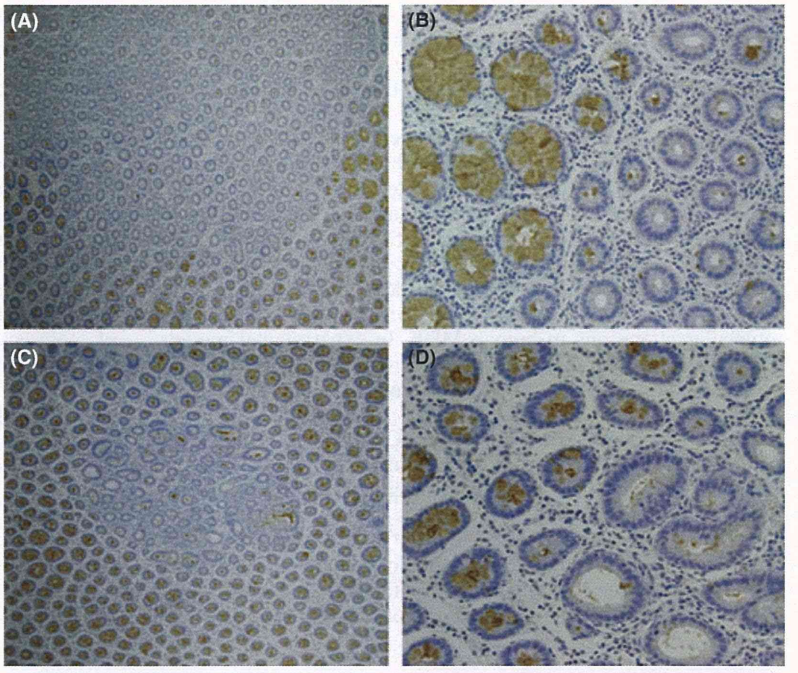

Fig. 2. Immunohistochemical staining for MUC2, which is the most abundant mucin in the colon, in the mucin-depleted foci (MDF) identified from sporadic CRC patients. Flat-MDF (A,B) and protruded-MDF (C,D) showing decrease/loss of goblet cells and MUC2 expression as compared with the surrounding crypts.

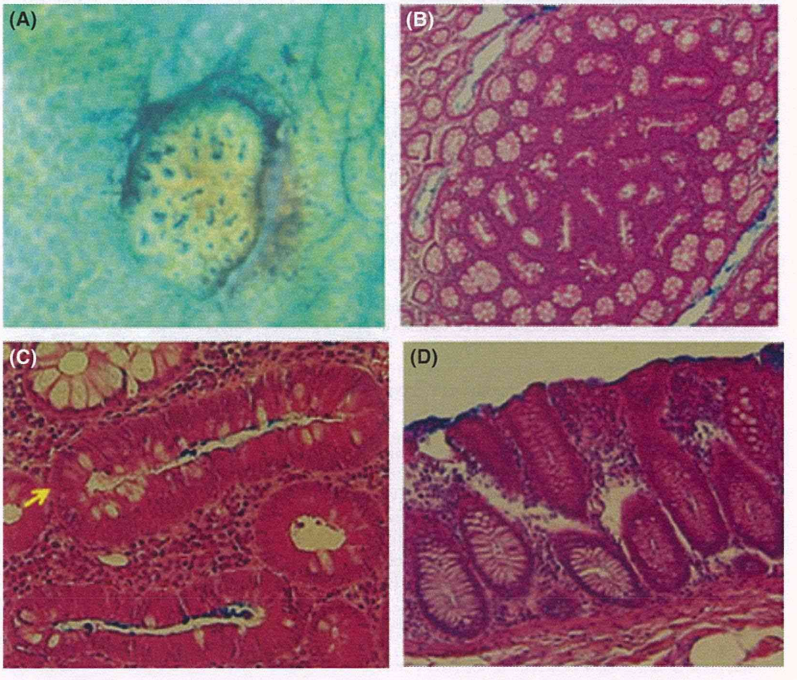

Fig. 3. The correspondence of mucin-depleted foci (MDF) in a patient with familial adenomatous polyposis (FAP). MDF formed by 30 crypts in AB-stained sections (A), and the corresponding HE-stained en-face (B,C), and longitudinal preparations (D). All MDF (eight lesions) identified in the FAP patient were flat-type and showed slight nuclear stratification and loss of polarity, and also having Paneth cell metaplasia (arrow), corresponding to moderate-grade dysplasia.

patients; FAP patients carry germ-line mutations in the *APC*, and, therefore, accumulated gene mutations might promote progression from MDF to an advanced stage of colorectal carcinogenesis in humans. Furthermore, we found inflammatory cell infiltration as a specific histological feature of MDF. Although the significance of this inflammatory cell infiltration is not clear, it might be related to immune defenses or recognition of the new altered cell population. The most abundant mucin, MUC2, has been reported to be depleted in the colonic MDF in carcinogen-treated rats,[30] and it has been suggested that the lack of MUC2 protein activates inflammatory markers in MDF.[31] It has also been reported that genetically MUC2-deficient mice develop CRC spontaneously, as well as colitis.[32,33] In the case of humans, several studies have revealed diminished MUC2 mRNA expression in CRC patients.[34–36] These results indicate that the lack of a protective layer of mucus might activate local inflammation, and contribute to further progression of MDF to a more advanced stage of colorectal carcinogenesis in humans.

Although our study indicates that MDF might serve as preneoplastic lesions not only in experimental models, but also

in humans, there ae some limitations. AB staining with acidic solution is unsuitable for *in vivo* endoscopic identification of MDF in humans. In addition, the low prevalence of MDF in human sporadic CRC patients means that it is difficult to use them as surrogate biomarkers of CRC. Therefore, we could not show clinical usefulness of MDF immediately. However, MDF might be useful for select high-risk subjects who need frequent surveillance. In the future, to evaluate whether MDF have a robust correlation with future CRC development, we need to establish a method of endoscopic identification of these lesions with future technical progress of *in vivo* visualization or particular mucosal staining that enables the detection of MDF. Moreover, in this study, we did not evaluate the genetic and molecular alterations in human MDF. In experimental models, MDF has been reported to show nuclear stratification and loss of polarity,[21] and activation of Wnt signaling, driven in part by mutations of the β-catenin and *Apc* genes.[17,37] In contrast, human MDF identified in sporadic CRC patients does not show nuclear stratification and loss of polarity. The primary mechanisms of colorectal carcinogenesis in carcinogen-treated rodent models are the frequent gene mutations of β-catenin and altered cellular localization of the protein.[38,39] However, stabilizing mutations of β-catenin in the absence of mutations of the *APC* have been described in only approximately 7% of sporadic CRC patients.[40] This might have an important implication in the different histological characteristics of MDF between humans and experimental rodent models. To elucidate the relevance of human MDF in colorectal carcinogenesis, further study of the underlying genetic and molecular alterations is needed.

In conclusion, we confirmed that MDF can also be identified in sporadic CRC patients just as in carcinogen-treated rodent models. We demonstrated that these lesions show histological features corresponding to low-grade dysplasia and are characterized by the specific histopathological characteristics of Paneth cell metaplasia and inflammatory cell infiltration. These characteristics have been demonstrated to be associated with an increased risk of CRC development. Thus, MDF in humans might represent an early-step histological change in the process of colorectal carcinogenesis, and could probably serve as preneoplastic lesions of CRC.

Acknowledgments

This work was supported in part by a Grant-in-Aid from the Ministry of Education, Culture, Sports, Science and Technology of Japan and a Grant-in-Aid from the Ministry of Health, Labour and Welfare.

Disclosure Statement

No potential conflict of interests to disclose.

References

1 Winawer SJ, Zauber AG, Ho MN *et al.* Prevention of colorectal cancer by colonoscopic polypectomy. The National Polyp Study Workgroup. *N Engl J Med* 1993; **329**: 1977–81.
2 Jemal A, Siegel R, Xu J. Cancer statistics 2010. *CA Cancer J Clin* 2010; **57**: 43–66.
3 Bertagnolli MM, Eagle CJ, Zauber AG *et al.* Celecoxib for the prevention of sporadic colorectal adenomas. *N Eng J Med* 2006; **355**: 873–84.
4 Bird RP. Observation and quantification of aberrant crypts in the murine colon treated with a colon carcinogen: preliminary findings. *Cancer Lett* 1987; **37**: 147–51.
5 McLellan EA, Bird RP. Specificity study to evaluate induction of aberrant crypts in murine colons. *Cancer Res* 1998; **48**: 6183–6.
6 McLellan EA, Bird RP. Aberrant crypts: potential preneoplastic lesions in the murine colon. *Cancer Res* 1988; **48**: 6187–92.
7 McLellan EA, Medline A, Bird RP. Dose response and proliferative characteristics of aberrant crypt foci: putative preneoplastic lesions in rat colon. *Carcinogenesis* 1991; **12**: 2093–8.
8 McLellan EA, Medline A, Bird RP. Sequential analyses of the growth and morphological characteristics of aberrant crypt foci: putative preneoplastic lesions. *Cancer Res* 1991; **51**: 5270–4.
9 McLellan E, Bird RP. Effect of disulfiram on 1,2-dimethylhydrazine-and azoxymethane-induced aberrant crypt foci. *Carcinogenesis* 1991; **12**: 969–72.
10 Pretlow TP, Barrow BJ, Ashton WS *et al.* Aberrant crypts: putative preneoplastic foci in human colonic mucosa. *Cancer Res* 1991; **51**: 1564–7.
11 Takayama T, Katsuki S, Takahashi Y *et al.* Aberrant crypt foci of the colon as precursors of adenoma and cancer. *N Engl J Med* 1998; **339**: 1277–84.
12 Hurlstone DP, Cross SS. Role of aberrant crypt foci detected using high-magnification-chromoscopic colonoscopy in human colorectal carcinogenesis. *J Gastroenterol Hepatol* 2005; **20**: 173–81.
13 Seike K, Koda K, Oda K *et al.* Assessment of rectal aberrant crypt foci by standard chromoscopy and its predictive value for colonic advanced neoplasms. *Am J Gastroenterol* 2006; **101**: 1362–9.
14 Mutch MG, Schoen RE, Fleshman JW *et al.* A multicenter study of prevalence and risk factors for aberrant crypt foci. *Clin Gastroenterol Hepatol* 2009; **7**: 568–74.
15 Caderni G, Femia AP, Giannini A *et al.* Identification of mucin-depleted foci in the unsectioned colon of azoxymethane-treated rats: correlation with carcinogenesis. *Cancer Res* 2003; **63**: 2388–92.
16 Femia AP, Dolara P, Caderni G. Mucin-depleted foci (MDF) in the colon of rats treated with azoxymethane (AOM) are useful biomarkers for colon carcinogenesis. *Carcinogenesis* 2004; **25**: 277–81.
17 Femia AP, Bendinelli B, Giannini A *et al.* Mucin-depleted foci have β-catenin gene mutation, altered expression of its protein, and are dose- and time-dependent in the colon of 1,2-dimethylhydrazine-treated rats. *Int J Cancer* 2005; **116**: 9–15.
18 Arikawa AY, Gallaher DD. Cruciferous vegetables reduce morphological markers of colon cancer risk in dimethylhydrazine-treated rats. *J Nutr* 2008; **138**: 526–32.
19 Femia AP, Giannini A, Fazi M *et al.* Identification of mucin depleted foci in the human colon. *Cancer Prev Res* 2008; **1**: 562–7.
20 Rex DX, Kahi CJ, Levin B *et al.* Guidelines for colonoscopy surveillance after cancer resection: a consensus update by the American Cancer Society and the US Multi-Society Task Force on Colorectal Cancer. *Gastroenterology* 2006; **130**: 1865–71.
21 Yoshimi N, Morioka T, Kinjo T *et al.* Histological and immunohistochemical observations of mucin-depleted foci (MDF) stained with Alcian blue, in rat colon carcinogenesis induced with 1,2-dimethylhydrazine dihydrochloride. *Cancer Sci* 2004; **95**: 792–7.
22 Roncucci L, Pedroni L, Vaccina F *et al.* Aberrant crypt foci in colorectal carcinogenesis. *Cell Crypt Dynamics Cell Prolif* 2000; **33**: 1–18.
23 Roncucci L, Medline A, Bruce WR. Classification of aberrant crypt foci and microadenomas in human colon. *Cancer Epidemiol Biomarkers Prev* 1991; **1**: 57–60.
24 Yamashita N, Minamoto T, Ochiai A *et al.* Frequent and characteristic K-ras activation and absence of p53 protein accumulation in aberrant crypt foci of colon. *Gastroenterology* 1995; **108**: 434–40.
25 Otori K, Sugiyama K, Hasebe T *et al.* Emergence of adenomatous aberrant crypt foci (ACF) from hyperplastic ACF with concomitant increase in cell proliferation. *Cancer Res* 1995; **55**: 4743–6.
26 Roncucci L, Modica S, Pedroni M *et al.* Aberrant crypt foci in patients with colorectal cancer. *Br J Cancer* 1998; **77**: 2343–8.
27 Rosenberg DW, Yang S, Pleau DC *et al.* Mutations in BRAF and KRAS differentially distinguish serrated versus non-serrated hyperplastic aberrant crypt foci in humans. *Cancer Res* 2007; **67**: 3551–4.
28 Sakai E, Takahashi H, Kato S, Uchiyama T, Hosono K *et al.* Investigation of the prevalence and number of aberrant crypt foci associated with human colorectal neoplasm. *Cancer Epidemiol Biomarkers Prev* 2011; **20**: 1918–24.
29 Bansal M, Fenoglio CM, Robboy SJ, King DW. Are metaplasias in colorectal adenomas truly metaplasias? *Am J Pathol* 1984; **115**: 253–65.
30 Femia AP, Tarquini E, Salvadori M *et al.* K-ras mutations and mucin profile in preneoplastic lesions and colon tumors induced in rats by 1,2-dimethylhydrazine. *Int J Cancer* 2008; **122**: 117–23.
31 Femia AP, Dorare P, Luceri C *et al.* Mucin-depleted foci show strong activation of inflamatory markers in 1,2-dimethylhydrazine-induced carcinogenesis and promoted by the inflammatory agent sodium dextran sulfate. *Int J Cancer* 2009; **125**: 541–7.
32 Velcich A, Heyer J, Fragale A *et al.* Colorectal cancer in mice genetically deficient in the mucin MUC2. *Science* 2002; **295**: 1726–9.
33 Van der Sluis M, De Koning BA, De Bruijn AC *et al.* Muc2-deficient mice spontaneously develop colitis, indicating that MUC2 is critical for colonic protection. *Gastroenterology* 2006; **131**: 117–29.

doi: 10.1111/j.1349-7006.2011.02125.x

34 Ogata S, Uehara H, Chen A *et al.* Mucin gene expression in colonic tissues and cell lines. *Cancer Res* 1992; **52**: 5971–8.
35 Ho SB, Niehans GA, Lyftogt C *et al.* Hetegeneity of mucin gene expression in normal and neoplastic tissues. *Cancer Res* 1993; **53**: 641–51.
36 Blank M, Klussman E, Kruger-Krasagakes S *et al.* Expression of MUC2-mucin in colorectal adenomas and carcinomas of different histological types. *Int J Cancer* 1994; **59**: 301–6.
37 Femia AP, Dolara P, Giannini A *et al.* Frequent mutation of Apc gene in rat colon tumors and mucin depleted foci, preneoplastic lesions in experimental colon carcinogenesis. *Cancer Res* 2007; **67**: 445–9.
38 Takahashi M, Fukuda K, Sugiyama T *et al.* β-catenin is frequently mutated and demonstrates altered cellular localization in azoxymethane-induced rat colon tumors. *Cancer Res* 1998; **58**: 42–6.
39 Takahashi M, Mutoh M, Kawamori T *et al.* Altered expression of β-catenin, inducible nitric oxide synthase and cyclooxygenase-2 in azoxymethane-induced rat colon carcinogenesis. *Carcinogenesis* 2000; **21**: 1319–27.
40 Morin PJ, Sparks AB, Korinek V *et al.* Activation of beta-catein-Tcf signaling in colon cancer by mutations in beta-catenin or APC. *Science* 1997; **275**: 1787–90.

Pre-neoplastic lesion, mucin-depleted foci, reveals *de novo* high-grade dysplasia in rat colon carcinogenesis

CHANGXU CUI[1,2], REIKA TAKAMATSU[1], HIROSHI DOGUCHI[1], AKIKO MATSUZAKI[1], MASANAO SAIO[1] and NAOKI YOSHIMI[1]

[1]Department of Pathology and Oncology, Graduate School of Medical Science, University of the Ryukyus, Okinawa, Japan; [2]Department of Biochemistry and Molecular Biology, Yanbian University Health Science Center, Yanji, P.R. China

Received November 9, 2011; Accepted December 23, 2011

DOI: 10.3892/or.2012.1657

Abstract. Aberrant crypt foci (ACF) and mucin-depleted foci (MDF) have recently been recognized as pre-neoplastic lesions in the colon of carcinogen-treated rodents. In the present study, we analyzed the sequential development of ACF and MDF histopathologically in the colon of rats from 5 to 40 weeks after DMH treatment. The numbers of ACF per colon increased over time during the experiment, and were much higher than the number in tumors, while the number of MDF per colon remained unchanged from the early stage (the 5th week after carcinogen exposure), and approximate to those in tumors. The incidence of ACF, which was much higher than that of tumors, also increased gradually in a time-dependent manner. The incidence of MDF, however, was similar to that of tumors and did not change significantly during the whole experiment. No lesion as dysplasia with high-grade (DHG) or adenocarcinoma (AC) were found in any large ACF from the 5th to 40th week histopathologically, whereas all of the large MDF showed DHG or AC features. Even at 5 weeks, MDF showed features of DHG. We classified these into two forms of MDF: flat and protruded MDF. At 40 weeks, the number of flat MDF per colon decreased significantly compared with that at 20 weeks ($p<0.05$), however, the number of protruded MDF per colon increased ($p<0.01$), and the percentage of DHG in a protruded MDF lesion decreased but that of AC increased remarkably. In conclusion, MDF may develop into cancer through the so-called '*de novo* cancer' pathway.

Correspondence to: Dr Changxu Cui, Department of Pathology and Oncology, Graduate School of Medical Science, University of the Ryukyus, Nishihara, Okinawa 903-0125, Japan
E-mail: xu9659@mail.ryudai.jp

Abbreviations: ACF, aberrant crypt foci; MDF, mucin-depleted foci; DMH, 1,2-dimethylhydrazine dihydrochloride; BCAC, β-catenin accumulated crypts; HPLL, hyperplastic polyp-like lesion; DLG, dysplasia (intraepithelial) with low-grade; DHG, dysplasia (intraepithelial) with high-grade; AC, adenocarcinoma

Key words: colon carcinogenesis, pre-neoplastic lesions, mucin-depleted foci

Introduction

Colon carcinogenesis occurs through consecutive steps, from normal crypt into pre-neoplastic lesion, adenoma, and finally change into carcinoma (1). In this process, the formation of early neoplastic lesions with various degrees of dysplasia is a crucial point. Accordingly, many efforts have been devoted to the identification and characterization of such lesions (2-5). Aberrant crypt foci (ACF), which was initially identified topographically on the colonic mucosa of rodents exposed to colorectal carcinogens, have been believed as a pre-neoplastic lesion in many studies of chemoprevention. Actually, the simple identification of ACF in experiments is very useful and important as a biomarker, because it does not need histopathological knowledge. Furthermore, a similar lesion has been also observed in humans. The association between ACF and development of colonic neoplasia has been described both in rodents and human (2,4,6,7). In contrast, there are several studies, which show lack of association between ACF and development of colonic neoplasms (8-10).

Previously, we have proposed β-catenin accumulated crypts (BCAC) as one of more predictive biomarkers in rat colon carcinogenesis (11,12). However, the identification require histological steps and immunohistochemistry. Recently, mucin-depleted foci (MDF) have been described to be the pre-neoplastic lesion which could be used as biomarkers in colon carcinogenesis. MDF were also identified in colon mucosa at high risk of colon cancer in human (8,13,14). The identification of MDF is relatively simple and examined topographically on the colonic mucosa with mucin staining instead of methylene bleu staining as well as ACF. We also reported that MDF has similar characteristics to BCAC rather than ACF (15), but there are no reports on the sequential histopathological analyses of MDF to our knowledge.

In the present study we examined the sequential development of ACF and MDF in the colon of rats from 5 to 40 weeks after DMH treatment. In order to identify early lesions with a morphological and developmental relationship with tumorigenesis, we classified the developing lesions by surface examination, quantified them, determined their growth and examined them sequentially and histopathologically.

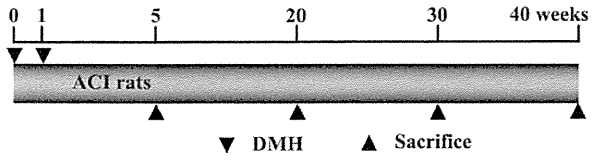

Figure 1. Experimental design. The rats were treated by subcutaneous injection of DMH with a dose of 40 mg/kg body weight, once a week for 2 weeks. At different times after DMH (arrows) rats were sacrificed.

Materials and methods

Animals and treatments. Four-week-old male ACI rats were obtained from Japan SLC, Inc. (Hamamatsu, Japan). All animals were housed in wire cages (3 rats/cage) with free access to drinking water and a basal diet, CE-2 (CLEA Japan, Inc., Tokyo), under controlled conditions of humidity (50±10%), lighting (12-h light/dark cycle) and temperature (23±2°C). DMH was purchased from Sigma-Aldrich Chemical Co. (St. Louis, MO). This study was approved by the Animal Welfare Committee of the University of the Ryukyus.

Experimental protocol. Experimental protocol is shown in Fig. 1. In brief, after quarantine for 1 week, the experiment was started at 5 weeks of age, the rats were treated by subcutaneous injection of DMH with a dose of 40 mg/kg body weight, once a week for 2 weeks. At 5, 20, 30 and 40 weeks after the first DMH treatment, rats were sacrificed under CO_2 anesthesia. Immediately after sacrifice, the colons were removed, and fixed in 10% buffered formalin.

Identification of ACF and MDF in unsectioned colon. Alcian blue staining was used to identify both ACF and MDF, instead of the conventional staining using 0.2% methylene blue and high-iron diamine Alcian blue, respectively (2,8). Briefly, the fixed colons were rinsed for 5 min in 3% acetic acid and then stained for 5 min with 1% Alcian blue solution (pH 2.5) in 3% acetic acid. These colons were rinsed for 5 min in 3% acetic acid to prevent non-specific staining and then washed in distilled water (15). ACF were identified according to the following criteria: larger than the adjacent normal crypts and elevated with thickened cell wall lining the crypt and increased pericryptal area and multiplicity (i.e., the number of crypts forming each focus) higher than 4 crypts (Fig. 2A), in accordance with other studies using methylene blue staining (2), in addition to crypts with mucous production. MDF were identified as focal lesions by the following criteria: i) absence or very small production of mucins; ii) distortion of the opening of the lumen compared with normal surrounding crypts; iii) multiplicity higher than 4 crypts (8,15). MDF can be divided into two types according to morphological characteristics. One is flat paralleled with normal mucosa; the other is protruded as crypts expanding and swelling over normal mucosa. Both types are judged as negative in Alcian blue staining. The latter looks like ACF in conventional methylene blue staining, it was described as overlapping lesion in a previous study (15). We herewith classified and counted MDF with a flat lesion (a flat MDF, Fig. 2B) and MDF with a protruded change (a protruded MDF, Fig. 2C), respectively. The stained mucosa including both ACF and MDF were photographed with a DP-50 digital camera (Olympus Optical Co., Ltd., Tokyo) and the positions of both lesions were marked on the captured images in a computer monitor. The numbers of MDF and ACF per colon were recorded. In addition, some ACF was also confirmed by conventional methylene blue staining.

Histopathological examinations. After the identification of ACF and MDF, they were embedded in paraffin for histological analyses. Colonic mucosal sections were examined by utilizing both an en face preparation (11) and a conventional vertical preparation for a half section of each lesion, respectively. Sections were stained with hematoxylin and eosin (H&E). The computer-captured images including ACF and MDF in unsectioned colons were compared with the histological lesions in the sections. The histopathological diagnoses of the lesions were defined as four types: i) hyperplastic polyp-like lesion (HPLL); ii) dysplasia (intraepithelial neoplasia) with low-grade (DLG); iii) dysplasia (intraepithelial neoplasia) with high-grade (DHG); iv) adenocarcinoma (AC), according to the criteria (16-19) with our modification by decrease or loss of goblet cells, the crypt structure, and the nuclear abnormalities (Fig. 3).

Statistical analysis. Data are presented as mean ± SE. Student's t-test was used to determine the significance of differences between groups. P-values <0.05 were considered to be significant.

Results

Identification of ACF and MDF. Although numbers of ACF per colon were increased in a time-dependent manner, those of MDF including flat and protruded types kept relatively stable. At 20 weeks, the numbers of ACF and MDF were 24.17±2.1 and 0.5±0.15, respectively. Although the numbers of ACF showed significantly higher than those in tumors at 40 weeks (0.8±0.27), those of MDF were not significantly different from those of tumors, i.e. >3 mm in size macroscopically at sacrifice (Fig. 4A and B). Incidence of ACF gradually increased together with time, while that of MDF was relatively stable. At 20 weeks, the incidence of ACF and MDF were 100 and 50%, respectively. At 40 weeks, the incidence of MDF was approximate to that in tumors (45%) (Fig. 4C). Then we evaluated the time-dependent changes of the numbers of both flat and protruded MDF with more than 4 crypts. The numbers per colon and incidence of both flat and protruded MDF were stable until 20 weeks (Fig. 5A and B). At 40 weeks, the end of the experiment, the numbers of a flat MDF showed a significant reduction ($p<0.05$), while those of a protruded MDF were up-regulated ($p<0.01$).

Histopathological features corresponding to ACF and MDF. Representative micro-stereoscopic and histological findings of ACF and MDF within 4 crypts in early stage (Fig. 6A-F) and with more than 10 crypts in late stages (Fig. 6G-L) was demonstrated. ACF consisted of HPLL (54.5%) and DLG (45.5%) histopathologically, while in MDF, 62.1% was DHG

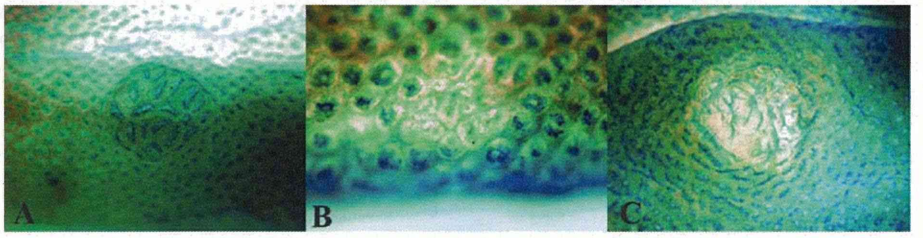

Figure 2. Morphological appearance of each lesion in the rat colon stained with Alcian blue staining. (A) ACF; (B) a flat MDF; (C) a protruded MDF. Original magnification, x40 in ACF and protruded MDF; x100 in MDF.

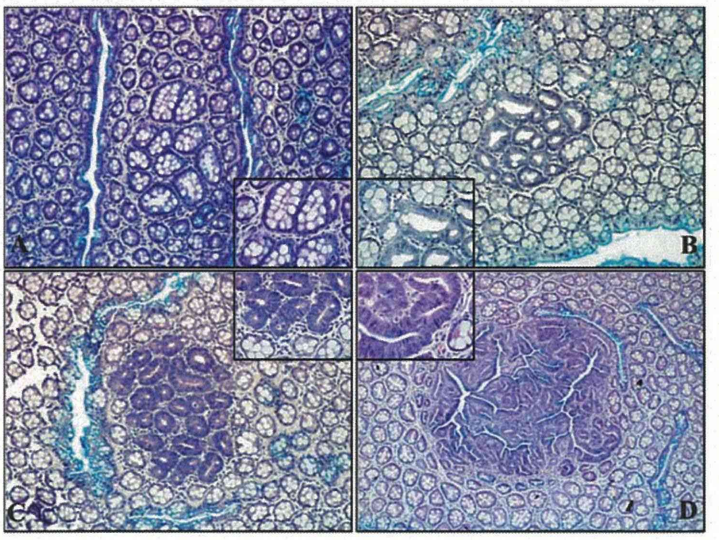

Figure 3. Histopathological findings of each classification of the pre-neoplastic or neoplastic lesions. (A) Hyperplastic polyp-like lesion; (B) dysplasia (intraepithelial), low grade; (C) dysplasia (intraepithelial), high grade; (D) adenocarcinoma. Original magnification, x100.

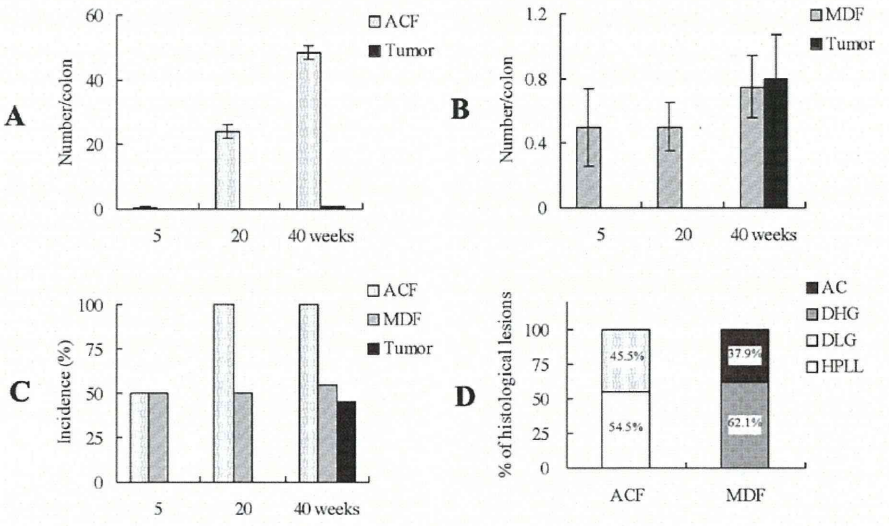

Figure 4. The sequential development of ACF and MDF in the colon of rats from 5 to 40 weeks after DMH treatment. (A) The number of ACF per colon increased over time during the experiment, and was much more than the number in tumors; (B) the number of MDF per colon remained unchanged from the early stage, and approximate to that in the tumor; (C) the incidence of ACF, which was much higher than that in the tumor. The incidence of MDF was similar to that in the tumor during the whole experiment; (D) no DHG was found in any large ACF from the 5th to 40th week in the experiment, whereas all of the large MDFs showed DHG or adenocarcinoma. Values represent mean ± SE.

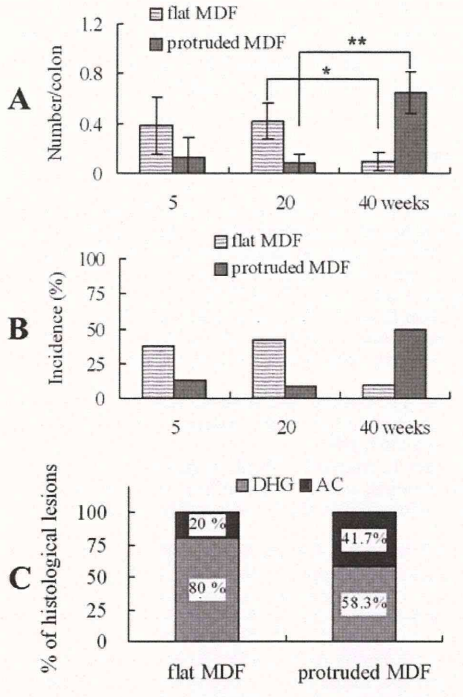

Figure 5. The sequential development of flat MDF and protruded MDF in the colon of rats from 5 to 40 weeks after DMH treatment. (A) In the 40 weeks, number of a flat MDF per colon decreased significantly compared with that in the 20 weeks, but number of a protruded MDF per colon increased; (B) at the level of incidence, flat MDF and protruded MDF was also similar to process of changes in number; (C) in histopathology, in contrast with flat MDF, the percentage of DHG in a protruded MDF decreased but that of AC increased remarkably. Values represent mean ± SE. $^{*}p<0.05$, $^{**}p<0.01$.

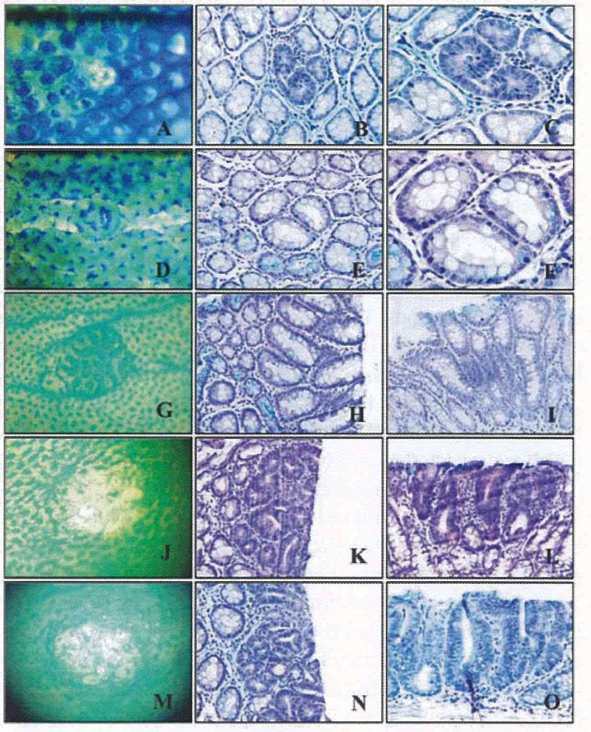

Figure 6. Representative features of the examined small lesions at 5 week (A-F). (A-C) MDF in AB staining (A) the corresponding H&E-stained lesion (B and C); (D-F) ACF in AB staining (D) the corresponding H&E-stained lesion (E and F). Representative of the examined large lesions (more than 10 crypts) at late stage in AB staining the corresponding H&E-stained lesion by en face preparation and a vertical preparation, respectively (G-O). (G-I) ACF; (J-L) a flat MDF; (M-O) a protruded MDF.

and 37.9% was AC. In the ACF, there was no malignancy. All MDF have malignant potential (Fig. 4D). Then we analyzed the histopathological difference between flat and protruded MDF. In a flat MDF, 80% was DHG, 20% was AC and 58.3% was DHG, while 41.7% was AC in a protruded MDF. The percentage of DHG in a protruded MDF was obviously lower than that in a flat MDF. In contrast, the percentage of AC in a protruded MDF was increased compared with that in a flat MDF (Fig. 5C).

Discussion

In this study, we observed the sequential and histopathological changes of MDF in detail, which is reported as one of useful biomarkers in animal colon carcinogenesis by Caderni *et al* (8). It showed that the numbers of ACF per colon increased together with the experimental duration, while those of MDF per colon were unchanged from early stage (at 5 weeks after carcinogen exposure) (Fig. 4A and B). The counted numbers of ACF were similar to the results of a previous study (20). Furthermore, the incidence of ACF also increased gradually in a time-dependent manner, but that of MDF did not significantly change (Fig. 4C). By histological examination, no DHG was found in any large ACF from the 5th to 40th week in the experiment, whereas all of the large MDF showed DHG or adenocarcinoma (Fig. 4D). Hence, our data suggest that MDF are histopathologically associated with more malignant potential than ACF.

MDF has been identified along the entire mucosal surface of unbedded colon as well as ACF (8). It is essential and important that MDF is related to colonic mucins. Mucins are highly glycosylated proteins that are the major components of the mucins that lubricate and protect the underlying intestinal epithelium (21). Although alterations of mucin expression and glycosylation have been observed in human colon cancer specimens (22), the role of these changes in the development of tumor has yet to be clarified. Moreover, it has been noted that sialomucin increased relatively due to a reduction of sulfomucin in colon cancer in human and rats (23-27). Therefore, Caderni *et al* used high-iron diamine Alcian blue staining, which can stain for sialomucin and sulfomucin respectively, for the detection of MDF (8). However, high-iron diamine Alcian blue staining is not convenient compared with methylene blue staining for ACF, and we used simple Alcian blue (pH 2.5) staining for MDF as described in our previous study (15), because a simple approach for the identification of mucin depletion might largely contribute to detect early malignancy.

Concerning ACF, there are several ACF such as classical and dysplastic ACF (28). Paulsen *et al* reported that the lesion defined as a flat ACF, which is recognized with methylene blue staining, seems like a useful biomarker in animal colon carci-

nogenesis (29,30). It looks like MDF, and actually, Femia *et al* collaborated to examine both lesions (31). In their study, over a half of both lesions are identical. Ochiai *et al* also defined a flat and dysplastic ACF by methylene blue staining (28,32). However, it is difficult and complex to compare the description of ACF lesions such as Paulsen and Ochiai, because the staining time and the staining patterns between the studies are quite different. Therefore, the same nomenclature as ACF might be confused. ACF, observed in this study, also is slightly different from the original ACF, because of our identification of ACF is dependent on the tissues with AB staining as described in Materials in methods. The most important issue in this study is to decrease the mucin of pre-neoplastic or neoplastic lesions as MDF and represent the characteristics of histological findings.

In this study, we have proposed a new classification of MDF such as a flat MDF and a protruded MDF. The latter, which we reported as overlapped lesion in our previous study (15), looks like topographical ACF appearance on the colonic mucosa. When we analyzed the two forms of MDF, such as a flat and a protruded MDF, numbers of both flat and protruded MDF per colon did not change by the end of 20th week. At 40 weeks, however, with formation of tumor, number of flat MDF per colon decreased significantly compared with that at 20 weeks, but the number of protruded MDF per colon increased (Fig. 5A). In histopathology, in contrast with flat MDF, the percentage of DHG in a protruded MDF decreased but that of AC increased remarkably (Fig. 5C). Our findings suggest that a flat MDF may transform into a protruded MDF gradually with time.

In addition, histopathological findings of MDF or BCAC at 5 weeks revealed high-grade adenoma with severe nuclear atypia (12,15), as well as those of Fig. 6B and C in this study. In this study, we diagnosed it as DHG according to the WHO classification (18). Our findings indicated that all of the small MDFs (less than 4 crypts) showed DHG histopathologically, and no AC was found in the early stage. But over time, AC appeared in the large MDFs (more than 10 crypts) during the late stage (Figs. 4D and 6K and L). As the differential diagnosis between adenoma and adenocarcinoma is usually done by the invasive characteristics (18,19), we diagnosed the tumors according to these criteria. However, in humans, the existence of 'intramucosal carcinoma' has been recognized indicating non-invasive cancer (18). In fact, many Japanese surgical/anatomic pathologists may recognize them as the feature of carcinoma *in situ*. This is a well known difference in the diagnosis of tumor of the gastrointestinal tract in humans between Western countries and Japan (33). According to Japanese criteria for colonic tumors, small MDF is close to the malignancy and *de novo* pathway in colon carcinogenesis.

In conclusion, MDF may develop into cancer through the so-called '*de novo* cancer' pathway histopathologically. However, it was difficult to distinguish large (dysplastic) ACF from protruded MDF even in this study. Further research on molecular changes in a protruded MDF, concerning '*de novo* cancer' is required.

Acknowledgements

This study was supported in part by a Grant-in-Aid from the Ministry of Education, Culture, Sports, Science and Technology of Japan and a Grant-in-Aid from the Ministry of Health, Labour and Welfare of Japan. We also acknowledge all members of our laboratories for the helpful comments and collaborations, especially Eriko Miyagi.

References

1. Chang WW: Histogenesis of colon cancer in experimental animals. Scand J Gastroenterol (Suppl) 104: 27-43, 1984.
2. Bird RP: Observation and quantification of aberrant crypts in the murine colon treated with a colon carcinogen: preliminary findings. Cancer Lett 37: 147-151, 1987.
3. McLellan EA, Medline A and Bird RP: Sequential analyses of the growth and morphological characteristics of aberrant crypt foci: putative preneoplastic lesions. Cancer Res 51: 5270-5274, 1991.
4. Pretlow TP, Barrow BJ, Ashton WS, *et al*: Aberrant crypts: putative preneoplastic foci in human colonic mucosa. Cancer Res 51: 1564-1567, 1991.
5. Roncucci L, Stamp D, Medline A, Cullen JB and Bruce WR: Identification and quantification of aberrant crypt foci and micro-adenomas in the human colon. Hum Pathol 22: 287-294, 1991.
6. Bird RP, McLellan EA and Bruce WR: Aberrant crypts, putative precancerous lesions, in the study of the role of diet in the aetiology of colon cancer. Cancer Surv 8: 189-200, 1989.
7. Fenoglio-Preiser CM and Noffsinger A: Aberrant crypt foci: a review. Toxicol Pathol 27: 632-642, 1999.
8. Caderni G, Femia AP, Giannini A, *et al*: Identification of mucin-depleted foci in the unsectioned colon of azoxymethane-treated rats: correlation with carcinogenesis. Cancer Res 63: 2388-2392, 2003.
9. Magnuson BA, Carr I and Bird RP: Ability of aberrant crypt foci characteristics to predict colonic tumor incidence in rats fed cholic acid. Cancer Res 53: 4499-4504, 1993.
10. Zheng Y, Kramer PM, Lubet RA, Steele VE, Kelloff GJ and Pereira MA: Effect of retinoids on AOM-induced colon cancer in rats: modulation of cell proliferation, apoptosis and aberrant crypt foci. Carcinogenesis 20: 255-260, 1999.
11. Yamada Y, Yoshimi N, Hirose Y, *et al*: Frequent beta-catenin gene mutations and accumulations of the protein in the putative preneoplastic lesions lacking macroscopic aberrant crypt foci appearance, in rat colon carcinogenesis. Cancer Res 60: 3323-3327, 2000.
12. Yamada Y, Yoshimi N, Hirose Y, *et al*: Sequential analysis of morphological and biological properties of beta-catenin-accumulated crypts, provable premalignant lesions independent of aberrant crypt foci in rat colon carcinogenesis. Cancer Res 61: 1874-1878, 2001.
13. Femia AP, Dolara P and Caderni G: Mucin-depleted foci (MDF) in the colon of rats treated with azoxymethane (AOM) are useful biomarkers for colon carcinogenesis. Carcinogenesis 25: 277-281, 2004.
14. Femia AP, Giannini A, Fazi M, *et al*: Identification of mucin depleted foci in the human colon. Cancer Prev Res (Phila) 1: 562-567, 2008.
15. Yoshimi N, Morioka T, Kinjo T, *et al*: Histological and immunohistochemical observations of mucin-depleted foci (MDF) stained with Alcian blue, in rat colon carcinogenesis induced with 1,2-dimethylhydrazine dihydrochloride. Cancer Sci 95: 792-797, 2004.
16. Schlemper RJ, Riddell RH, Kato Y, *et al*: The Vienna classification of gastrointestinal epithelial neoplasia. Gut 47: 251-255, 2000.
17. Rectum JSfCotCa: General Rules for clinical and Pathological Studies on Cancer of the Colon, Rectum and Anus. 7th edition, Revised Version. Kanehara Shuppan, Ltd., Tokyo, 2009.
18. Bosman FT, Carneiro F, Hruban RH and Theise ND: WHO Classification of Tumors of the Digestive System. International Agency for Research on Cancer, Lyon, 2010.
19. Ward JM: Morphogenesis of chemically induced neoplasms of the colon and small intestine in rats. Lab Invest 30: 505-513, 1974.
20. Femia AP, Bendinelli B, Giannini A, *et al*: Mucin-depleted foci have beta-catenin gene mutations, altered expression of its protein, and are dose- and time-dependent in the colon of 1,2-dimethylhydrazine-treated rats. Int J Cancer 116: 9-15, 2005.

21. Gendler SJ and Spicer AP: Epithelial mucin genes. Annu Rev Physiol 57: 607-634, 1995.
22. Kim YS, Gum J Jr and Brockhausen I: Mucin glycoproteins in neoplasia. Glycoconj J 13: 693-707, 1996.
23. Zusman I, Zimber A and Nyska A: Role of morphological methods in the analysis of chemically induced colon cancer in rats. Acta Anat (Basel) 142: 351-356, 1991.
24. Dawson PA, Patel J and Filipe MI: Variations in sialomucins in the mucosa of the large intestine in malignancy: a quantimet and statistical analysis. Histochem J 10: 559-572, 1978.
25. Filipe MI: Value of histochemical reactions for mucosubstances in the diagnosis of certain pathological conditions of the colon and rectum. Gut 10: 577-586, 1969.
26. Matsushita Y, Yamamoto N, Shirahama H, *et al*: Expression of sulfomucins in normal mucosae, colorectal adenocarcinomas, and metastases. Jpn J Cancer Res 86: 1060-1067, 1995.
27. Sandforth F, Heimpel S, Balzer T, Gutschmidt S and Riecken EO: Characterization of stereomicroscopically identified preneoplastic lesions during dimethylhydrazine-induced colonic carcinogenesis. Eur J Clin Invest 18: 655-662, 1988.
28. Ochiai M, Ushigome M, Fujiwara K, *et al*: Characterization of dysplastic aberrant crypt foci in the rat colon induced by 2-amino-1-methyl-6-phenylimidazo[4,5-b]pyridine. Am J Pathol 163: 1607-1614, 2003.
29. Paulsen JE, Namork E, Steffensen IL, Eide TJ and Alexander J: Identification and quantification of aberrant crypt foci in the colon of Min mice - a murine model of familial adenomatous polyposis. Scand J Gastroenterol 35: 534-539, 2000.
30. Paulsen JE, Knutsen H, Olstorn HB, Loberg EM and Alexander J: Identification of flat dysplastic aberrant crypt foci in the colon of azoxymethane-treated A/J mice. Int J Cancer 118: 540-546, 2006.
31. Femia AP, Paulsen JE, Dolara P, Alexander J and Caderni G: Correspondence between flat aberrant crypt foci and mucin-depleted foci in rodent colon carcinogenesis. Anticancer Res 28: 3771-3775, 2008.
32. Ochiai M, Watanabe M, Nakanishi M, Taguchi A, Sugimura T and Nakagama H: Differential staining of dysplastic aberrant crypt foci in the colon facilitates prediction of carcinogenic potentials of chemicals in rats. Cancer Lett 220: 67-74, 2005.
33. Schlemper RJ, Itabashi M, Kato Y, *et al*: Differences in the diagnostic criteria used by Japanese and Western pathologists to diagnose colorectal carcinoma. Cancer 82: 60-69, 1998.

The Prostate 72:533–541 (2012)

Organ Specific Gst-pi Expression of the Metastatic Androgen Independent Prostate Cancer Cells in Nude Mice

Taku Naiki,[1,2] Makoto Asamoto,[1]* Naomi Toyoda-Hokaiwado,[1] Aya Naiki-Ito,[1] Keiichi Tozawa,[2] Kenjiro Kohri,[2] Satoru Takahashi,[1] and Tomoyuki Shirai[1]

[1]*Department of Experimental Pathology and Tumor Biology, Nagoya City University, Graduate School of Medical Sciences, Nagoya, Japan*

[2]*Department of Nephro-urology, Nagoya City University, Graduate School of Medical Sciences, Nagoya, Japan*

BACKGROUND. Elucidating the mechanisms of metastasis in prostate cancer, particularly to the bone, is a major issue for treatment of this malignancy. We previously reported that an androgen-independent variant had higher expression of glutathione S-transferase pi (Gst-pi) compared with a parent androgen-dependent transplantable rat prostate carcinoma which was established from the transgenic rat for adenocarcinoma of the prostate (TRAP).

METHODS. A new cell line, PCai1, was established from the androgen-independent tumor and investigated its metastatic potential in nude mice. The tumorigenesis of PCai1 cells in vivo was studied by subcutaneous transplantations into nude mice. The growth in the micro-environment of the prostate was studied by orthotopic transplantation of PCai1 cells into nude mice. The metastatic potential of PCai1 cells was studied by tail vein injections. Effects of *Gst-pi* knocked down were analysis in PCai1 cells.

RESULTS. PCai1 frequently formed metastatic lesions in the lung and lymph nodes after orthotopic implantation in the prostate. Intravenous injections of PCai1, metastasis to lung and bone were obvious. PCai1 had strong expression for Gst-pi, therefore we tried knocked down *Gst-pi*. *Gst-pi*-siRNA in vitro significantly suppressed cell proliferation rate. In addition, high levels of intracellular reactive oxygen species (ROS) were recognized in the *Gst-pi* knockout.

CONCLUSIONS. Gst-pi expression of the prostate cancers are dependent on metastatic site, and that Gst-pi has an important role in adapting prostate cancer for growth and metastasis involving an alteration of ROS signals. *Prostate 72: 533–541, 2012.* © 2011 Wiley Periodicals, Inc.

KEY WORDS: **prostate cancer; metastasis; Gst-pi; rats; cell line**

INTRODUCTION

Prostate cancer is one of the most frequently diagnosed cancers in the Western world [1]. Because prostate cancer development is initially androgen dependent, the basic therapeutic strategy has been the deprivation of androgens [2]. However, most tumors ultimately relapse after a period of initial response to this therapy and progress to castration-resistant prostate cancer (CRPC), for which effective therapeutic procedures are extremely limited. Administration of docetaxel has been established as a new standard of chemotherapy for CRPC patients [3–5]. However, it is not curative, and optimal timing of administration remains controversial. Consequently, there is a need

Grant sponsor: Ministry of Education, Culture, Sports Science and Technology of Japan; Grant sponsor: Ministry of Health, Labor and Welfare of Japan; Grant sponsor: Ono Pharmaceutical Co., Ltd.

Disclosure: There are no potential conflicts of interest.

Naomi Toyoda-Hokaiwado's present address is Division of Genetics and Mutagenesis, National Institute of Health Sciences, Tokyo, Japan.

*Correspondence to: , Dr. Makoto Asamoto, MD, PhD, Department of Experimental Pathology and Tumor Biology, Nagoya City University, Graduate School of Medical Sciences, Kawasumi 1, Mizuho-cho, Mizuho-ku 467-8601, Nagoya, Japan.
E-mail: masamoto@med.nagoya-cu.ac.jp

Received 7 January 2011; Accepted 15 June 2011
DOI 10.1002/pros.21455
Published online 11 July 2011 in Wiley Online Library (wileyonlinelibrary.com).

for exploration of new therapeutic strategies targeting detailed molecular mechanisms for the development of castration resistance in prostate cancer.

The generation of suitable in vivo models is essential to gain a better understanding of the processes associated with the development and progression of prostate cancer [6,7]. We previously reported on the transgenic rat model for adenocarcinoma of the prostate (TRAP) model [8], which features the introduction of the SV40 T antigen (SV40 Tag) gene under probasin control. In this model, complete androgen-dependent prostate adenocarcinomas developed in 100% of animals by 15 weeks of age [8–10]. These tumors were transplantable into the subcutis of nude mice. The transplanted tumors expressing androgen receptor (AR) regressed soon after the mice were castrated, but resumed growth under androgen depletion 12 weeks later. As the sequential changes of the xenograft resemble the clinical behavior of prostate cancer, this model may provide an excellent system to study the mechanisms associated with castration-resistant progression of prostate cancer and to evaluate new modalities for CRPC [11]. The androgen-independent prostate tumors established under such an experimental condition were subjected to cDNA microarray analysis which showed that glutathione S-transferase pi (*Gst-pi*) was overexpressed compared to the androgen-dependent tumors. Glutathione S-transferase pi (*GST-pi*) was also found to be overexpressed in the androgen-independent prostate cancer cell line, PC3 [11]. The suppression of GST-pi expression by siRNA inhibited tumor growth after subcutaneous transplantation of PC3 cells in nude mice [11].

A major component involved in the maintenance of reduction-oxidation (redox) balance in the cell is the glutathione redox system. Methods of inactivating *GST-pi* had been identified in almost all of the prostate cancer cases examined by Nelson et al. [12]. Since then, many reports have described the relations between *GST-pi* and androgen-dependent prostate cancer, and loss of the expression of their promoter sequences by methylation was found as an early event in human prostate carcinogenesis [13,14]. Therefore, a sensitive balance appears to exist between the oxidant and antioxidant components of the cells and their regulatory mechanisms in developing a malignant state in prostate tissue.

Redox reactions that generate reactive oxygen species (ROS) such as hydrogen peroxide, superoxide, and hydroxyl-free radicals have been identified as important chemical mediators in the regulation of signal transduction processes involved in cell growth and differentiation and have been reviewed [15–17]. ROS content is relatively higher in prostate epithelial cells than in most other tissues [18]. Direct evidence linking ROS with an increase in tumor development in the prostate has been established [19,20]. Previous studies highlighted the altered pro-oxidant–antioxidant status in prostatic tissue, and also in cell lines where the imbalance between these antagonists played a major role in the initiation of prostate carcinogenesis [21]. However, only few reports are available that describes interactions between androgen-independent prostate cancer and ROS. Moreover, no report addressed the mechanism using a cell line with a high metastatic potential in vivo.

In the present study, new androgen-independent prostate cancer cells were established which metastasized when transplanted into nude mice. The expression and function of Gst-pi in each metastatic site of the androgen-independent prostate cancer cells were studied.

MATERIALS AND METHODS

A New Androgen-Independent Prostate Cancer Cell Line

Cultures were initiated by mechanical disruption of the androgen-independent prostate tumor in nude mice [11] followed by enzymatic digestion with trypsin for 24 hr at 37°C. The resulting cells were incubated in DMEM (Nissui, Tokyo, Japan) with 10% heat-inactivated fetal bovine serum (FBS) (Equitech-Bio, Kerrville, TX). After 10 months passage and incubation, the surviving cells were selected and the cells that had the SV40 Tag expressions by RT-PCR were subcloned. Furthermore, the surviving cells in the androgen depleted medium containing 10% charcoal-stripped- (CS-) FBS (Hyclone) were selected, and one of these cell lines, named PCai1, which was androgen-independent cell line in vitro was used in our experiments. All cell cultures were maintained at 37°C in a humidified incubator with an atmosphere of 5% CO_2/95% air.

In Vivo Tumor Growth

Six-week-old male KSN/nu-nu nude mice were obtained from Nippon SLC. Mice were maintained in plastic cages on hardwood chips in an air-conditioned, pathogen-free animal room at 22 ± 2°C and 50% humidity with 12:12 hr light/dark cycle. All animal experiments were performed under protocols approved by the Institutional Animal Care and Use Committee of Nagoya City University School of Medical Sciences.

Subcutaneous transplantation of PCai1 cells. The tumorigenesis of PCai1 cells in vivo was studied by

subcutaneous transplantations into nude mice. PCai1 cells were cultured in T-75 flasks to confluence, trypsinized, and enumerated. Under isoflurane anesthesia four mice were surgically castrated and after 3 days, 1×10^5 PCai1 cells were injected subcutaneously into four normal and four castrated mice. Tumor sizes were calculated every 2 weeks, and mice were sacrificed 10 weeks after the implantation.

Orthotopic transplantation of PCai1 cells. The growth in the microenvironment of the prostate was studied by orthotopic transplantation of PCai1 cells into nude mice. Under isoflurane anesthesia, 5 of 10 nude mice were surgically castrated. After 3 days, 5×10^5 PCai1 cells were implanted into the lateral lobe of the prostate in both castrated and non-castrated mice. Two mice of each group were sacrificed 2 weeks after the injection. The study was terminated until become when the mice appeared moribund. After sacrifice, the orthotopic growth of the tumor and metastases in the para-aortic and bilateral inguinal lymph nodes, lung and systemic bone tissues were investigated histopathologically, as well as performing immunohistochemical analyses for AR, SV40 Tag, and Gst-pi.

Tail vein injection of PCai1 cells. The metastatic potential of PCai1 cells was studied by tail vein injections. Seven $\times 10^6$ cells were injected into the tail veins of 10 mice under anesthesia. At 5 and 9 weeks after the injections, the mice were sacrificed and the metastases in the para-aortic and bilateral inguinal lymph nodes, lung and systemic bone were investigated macroscopically and by immunohistochemical staining.

Histopathological Analysis

The transplants and metastatic tumors were fixed in 10% buffered formalin and embedded in paraffin. For bone metastases, specimens were treated with sterile decalcification solution for 48 hr prior to paraffin embedding. Serial (4 μm thick) sections were prepared. For immunohistochemical analysis, deparaffinized sections of the tissues were incubated with 1:1,000 diluted anti-Gst-pi (MBL, Nagoya, Japan), 1:100 diluted anti-AR (Santa Cruz Biotechnology, Inc., CA), 1:500 diluted SV40 Tag antibody (PharMingen, San Diego, CA). Antibody binding was visualized by a conventional immunostaining method using an autoimmunostaining apparatus (HX System, Ventana, Tucson, AZ).

RNA Preparation and Quantitative RT-PCR for Gst-pi and Gapdh

Total RNA was extracted using Isogen (Nippon Gene, Tokyo, Japan). One microgram sample was converted to complementary DNA with avian myoblastosis virus reverse transcriptase and oligo dT primers (TaKaRa, Otsu, Japan) in 20 μl of reaction mixture and 2 μl aliquots were subjected to quantitative polymerase chain reaction in 20 μl reactions using SYBR Premix Ex Taq™ (TaKaRa) and a Light Cycler apparatus (Roche Diagnostics, Mannheim, Germany). The fluorescence intensity of double-strand-specific SYBR Green 1, reflecting the amount of formed polymerase chain reaction product, was monitored at the end of each elongation step. Cyclophilin messenger RNA levels were employed to normalize for the 5′ sample complementary DNA content. Primer sequences for rat *Gst-pi* were 5′-GCTCTTT-AGGGCTTTATGGG-3′ and 5′-CTGTTTACCATT-GCCGTTGA-3′, and 5′-GCATCCTGCACCACCAA-CTG-3′ and 5′-GCCTGCTTCACCACCTTCTT-3′ for glyceraldehyde-3-phosphate dehydrogenase (*Gapdh*). Initial denaturation was at 95°C for 5 sec, annealing was at 55°C for 15 sec, and subsequently elongation was at 72°C for 30 sec. Gapdh mRNA levels were used for normalizing the sample cDNA content of PCai1 cells.

siRNA Transfection and Cell Growth Assay In Vitro

Stealth Select RNAi targeting rat *Gst-pi* sequences were obtained from Invitrogen. PCai1 cells (2×10^5) were seeded in six-well plates and transfected with 30 nM siRNA using LipofectAMINE RNAiMAX (Invitrogen) according to the manufacturer's protocol. Silencer negative control #1 siRNA (Invitrogen) with no significant homology to any known rat genes was used as a negative control siRNA. The ability of siRNA to silence the expression level of *Gst-pi* mRNA was checked on the second day after transfection. For monitoring growth inhibition, cells were trypsinized ($n = 4$) on days 3 and 5, and then the cell numbers were counted.

In Vivo Tumor Growth Analysis by Using siRNA for *Gst-pi*

Twenty-four hours after *Gst-pi* siRNA transfection by lipofectamine in T-75 flask, PCai1 cells were trypsinized and suspended in the DMEM media without serum, and 1×10^5/mouse cells were injected subcutaneously into five normal and five castrated nude mice. Negative control siRNA treated cells were also injected into normal and castrated mice for controls. Tumor volume was calculated every week, and 3 weeks after inoculation, the four groups of mice

were sacrificed and the final tumor volumes were measured in each group.

Western Blotting for Gst-pi and AR

Cells were lysed in SDS buffer and 10 μl were resolved on 12% polyacrylamide gels and transferred to Hybond ECL (GE Healthcare). Gst-pi and AR expression levels were assessed with the same antibody used for immunohistochemical staining. Beta actin expression was evaluated to confirm equal amount of protein loadings by monoclonal anti-beta-actin (Sigma, St. Louis, MO).

Cell Proliferation Assay After Dihydrotestosterone (DHT) Treatment

PCai1 cells were pretreated with medium containing CS-FBS for 2 weeks, and cell proliferation was measured in response to dihydrotestosterone (DHT) (Wako, Tokyo, Japan) treatments. PCai1 cells (5×10^4) were re-seeded in 96-well plates and treated with DHT from 10^{-5} to 10^5 nM in CS-FBS medium. Twenty-four hours after incubation, 10 μl/well of Cell Proliferation Reagent WST-1 (Roche, Basal, Switzerland) was added to the cells. Two hours after incubation, increase in fluorescence was measured by Spectrafluor Plus (Wako). The mean fluorescence intensity at 430 nm was calculated.

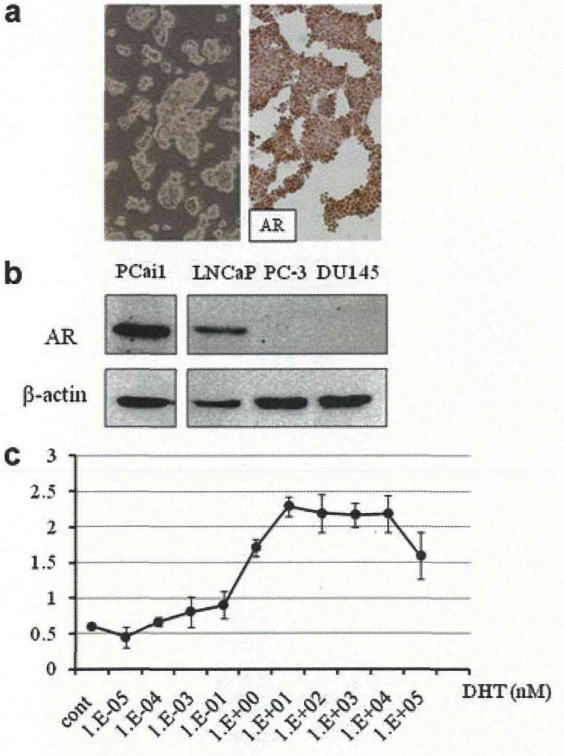

Fig. 1. Androgen receptor expression and function in PCai1 cell line. The established cell line, PCai1, grew with spheroid formation, and immunohistochemical analysis revealed intense nuclear staining for AR in androgen containing medium (**a**). Western blot analysis showed that PCai1 cells had AR expression similar to the human prostate cancer cell line LNCaP (**b**). WST-1 assay revealed that growth of PCai1 cells in CS-FBS medium was enhanced by 1–10 nM dihydrotestosterone (DHT) (**c**). [Color figure can be seen in the online version of this article, available at http://wileyonlinelibrary.com/journal/pros]

Measurement of Intracellular ROS Level

After pretreatment with DMEM without phenol red for 24 hr, 1×10^4 PCai1 cells were re-seeded in 96-well plates for 24 hr. The cells were then treated with 100 μg/ml 5-(and-6-)-chloromethyl-2′, 7′-dichlorodihydrofluorescein diacetate, acetyl ester (CM-H_2DCFDA) dye (Invitrogen). After 45 min incubation in the dark, levels of specific fluorescence were measured by Spectrafluor Plus. The data were normalized by the proliferation rate measured by the WST-1 assay.

Ethacrynic Acid Treatment in PCai1 Cells

To examine direct effects of Gst-pi on production of ROS or cell proliferation, PCai1 cells were treated with ethacrynic acid (EA) (Sigma), glutathione S-transferase pi inhibitor. Briefly, PCai1 cells were pretreated with phenol-free medium containing 10% FBS for 2 weeks, and cell proliferation and intracellular ROS were measured in response to EA treatments. PCai1 cells (1×10^5) were seeded in six-well plates, and exposed to 1 μM, 10 μM of EA. Cells were

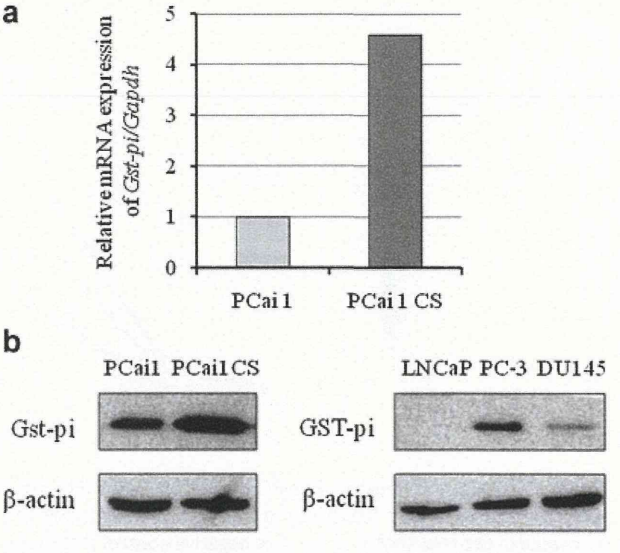

Fig. 2. Gst-pi expressions in PCai1. PCai1 in the CS-FBS medium (PCai1 CS) had higher expression levels of Gst-pi in RT-PCR (**a**) and Western blot (**b**) compared to cells in normal medium. Expressions of GST-pi in PC3 and DU145 were confirmed.

counted on days 3 and 5, and measurement of ROS level was performed as described above.

RESULTS

Establishment of an Androgen-Independent Prostate Cancer Cell Line

Our newly established androgen independent prostate cancer cell line, PCai1 (Fig. 1a), can survive in androgen-free DMEM with 10% CS-FBS. The cells showed intense nuclear immunohistochemical staining for AR in normal medium containing androgen (Fig. 1a). PCai1 and a human prostate cancer cell line LNCaP showed similar expressions of AR (Fig. 1b). The WST-1 assay revealed that cell growth was enhanced by 1–10 nM of DHT (Fig. 1c), so this cell line was androgen-independent and androgen-sensitive.

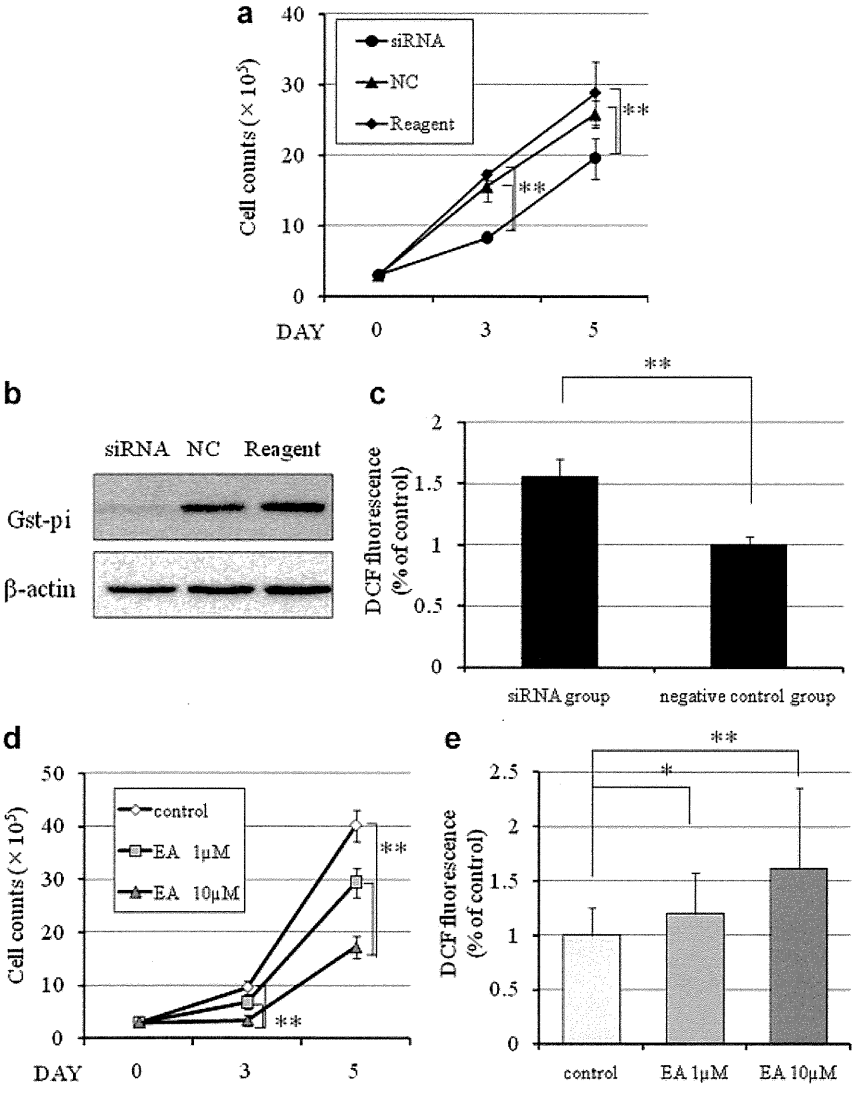

Fig. 3. Gst-pi siRNA treatment in PCai1 cells in CS-FBS medium. PCai1 cells in CS-FBS medium were treated with *Gst-pi*-siRNA. Significant growth inhibition ($^{**}P < 0.001$) was observed in the *Gst-pi*-siRNA treated PCai1 cells in CS-FBS medium (**a**). Gst-pi expression was markedly decreased in *Gst-pi*-siRNA group, while negative control (NC) group and reagent group had clearly detectable Gst-pi signals (**b**). DCFH assay revealed that ROS was significantly higher in *Gst-pi*-siRNA treatment group at day 3 after transfection ($^{**}P < 0.001$, **c**). At days 3 and 5, the numbers of PCai1 cells were counted after treatment with control, and 1 μM, 10 μM ethacrynic acid (EA). The suppression of proliferation was statistically significant by treatment of 1 or 10 μM ($^{**}P < 0.001$, **d**). DCFH assay revealed that the concentration dependence of ROS was higher in the EA treatment groups ($^{*}P < 0.05$, $^{**}P < 0.001$, **e**).

The Gst-pi Expression in PCai1 Cells

PCai1 cells in normal medium had stable expressions of Gst-pi in mRNA and protein levels. When PCai1 cells were cultured in CS-FBS medium, Gst-pi expressions were enhanced in mRNA and protein levels (Fig. 2). As reported previously [11], in human prostate cancer cells GST-pi expression was higher in the androgen-independent cell lines (PC3, DU145) compared with an androgen-dependent cell line (LNCaP). These results indicate that Gst-pi expression is higher in androgen-independent prostate cancer than those that are androgen-dependent.

Gst-pi siRNA Transfection and ROS Signals

To examine the role of Gst-pi expression for ROS signaling in PCai1 cells, *Gst-pi* expression was attenuated by RNAi. The suppression of proliferation of PCai1 cells in CS-FBS medium was statistically significant in *Gst-pi*-siRNA treated cells, but not in *Gst-pi*-negative control cells (Fig. 3a). Western blot analysis revealed Gst-pi protein expression has been inhibited by siRNA for 5 days after transfection (Fig. 3b). DCFH assay revealed that the intracellular ROS levels were significantly higher in the *Gst-pi*-siRNA treatment group than in *Gst-pi*-negative control group (Fig. 3c). Next, to examine whether Gst-pi directly affects modification of cell proliferation and production of ROS, PCai1 cells were treated with EA, a glutathione S-transferase pi inhibitor. As expected, proliferation of PCai1 was significantly inhibited by 1 and 10 μM EA compared with the non-treated control (Fig. 3d). Intracellular ROS levels were also significantly higher in the EA treatment group in a concentration-dependent manner (Fig. 3e).

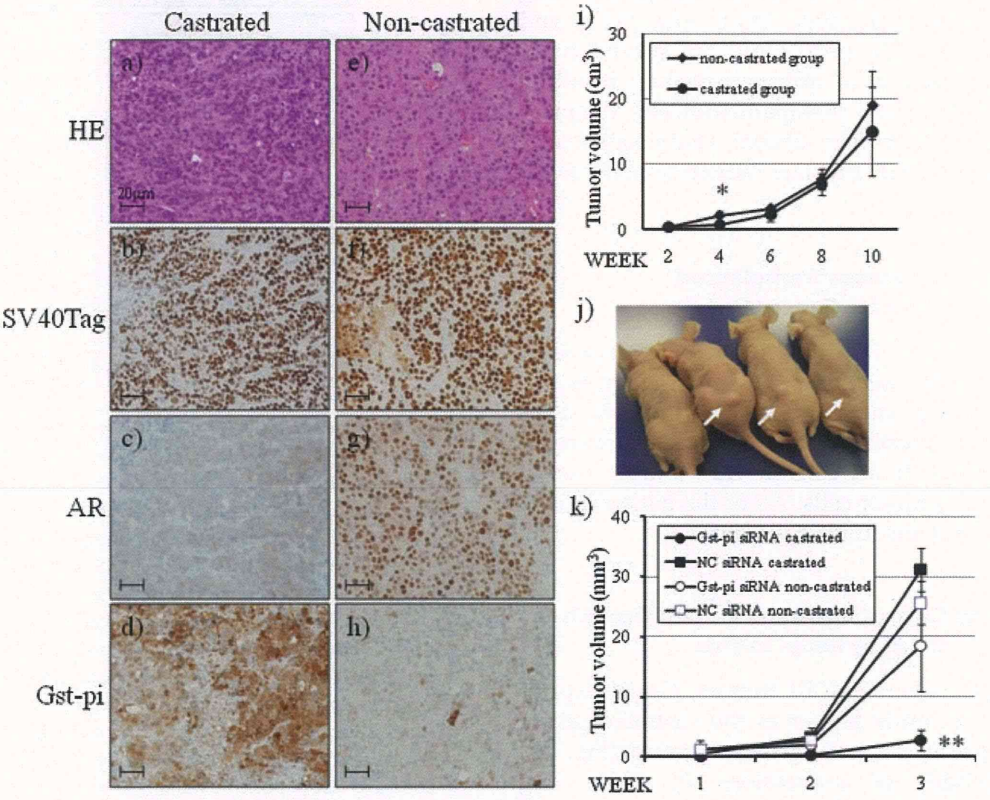

Fig. 4. Representative histopathological appearance of subcutaneous PCai1 tumor in nude mice. **a–d** shows the tumors in the castrated mice and **e–h** show the tumors in the non-castrated mice. SV40 Tag was stained to confirm origin from the TRAP prostate tumor (b,f). Non-castrated mice showed nuclear staining of AR (g), whereas castrated mice showed cytoplasmic staining (c), indicating non-active receptor function. The staining of Gst-pi was higher in castrated group (d) than in non-castrated group (h). The sequential changes are shown of subcutaneous PCai1 tumor volumes (**i**) (1×10^5 cells, n = 4 each, $^*P < 0.05$). Representative subcutaneous tumors at 2 weeks after injection in castrated or non-castrated groups (**k**, left: *Gst-pi* siRNA group with castration, second from the left: negative control siRNA group with castration, third from the left: *Gst-pi* siRNA group with non-castration, right: negative control siRNA group with non-castration, white arrow: tumor). **j**: Mean tumor volumes after subcutaneous injections (1×10^5 cells, n = 5 each). Interference of *Gst-pi* expression significantly inhibited tumor cell proliferation in castrated group compared with the corresponding negative control siRNA group ($^{**}P < 0.001$).

Prostate Cancer Subcutaneous Tumor Model

For investigation of tumorigenesis, PCai1 cells were transplanted subcutaneously in nude mice. Successful growth was seen in both castrated and non-castrated mice. The tumor sizes between the two groups lacked significance (Fig. 4i). Transplanted PCai1 cells had strong nuclear SV40 Tag expression, and demonstrated intense nuclear AR staining in the non-castrated group. In contrast, AR expression had changed from the nucleus to the cytoplasm in the castrated mice indicated not functional (Fig. 4a–h).

Prostate Cancer Orthotopic Transplanted Model

Whether or not they were castrated, the PCai1 cells grew in the prostate site in nude mice forming tumors which frequently metastasized to the lung and lymph nodes in nude mice (Fig. 5a–c and Table I). However, the mice could not survive more than 6 weeks because of urinary retention resulting from the tumor growth. Histopathologically, the prostate tumors in mice had similar characteristics as poorly differentiated prostate adenocarcinomas in human.

Intravenous Transplanted Prostate Cancer Cells

With injections of PCai1 cells into the tail veins of nude mice, metastatic tumors were frequently observed in the lungs and bones (Fig. 5g,h and Table I). Immunocytochemically, the SV40 Tag signals were intense in nuclei of PCai1 cells in vitro and in vivo of the metastasized tumor cells. All of the bone metastases were found in the lumbar vertebrae.

Regulation of Castration-Resistant Cell Growth of PCai1 by Gst-pi In Vivo

In the subcutaneous PCai1 tumors, Gst-pi expression was significantly higher in the castrated group (Fig. 4d) than in the non-castrated group (Fig. 4h) without changes in expressions of SV40 Tag (Fig. 4b,f). To evaluate roles of Gst-pi in castration-resistant cell proliferation, *Gst-pi* siRNA transfected PCai1 cells were transplanted subcutaneously in castrated or normal nude mice. Knock down of *Gst-pi* expression of PCai1 significantly inhibited tumor growth of PCai1 compared to negative controls in castrated mice. On the other hand, *Gst-pi* expression did not affect tumor growth in non-castrated mice (Fig. 4j,k).

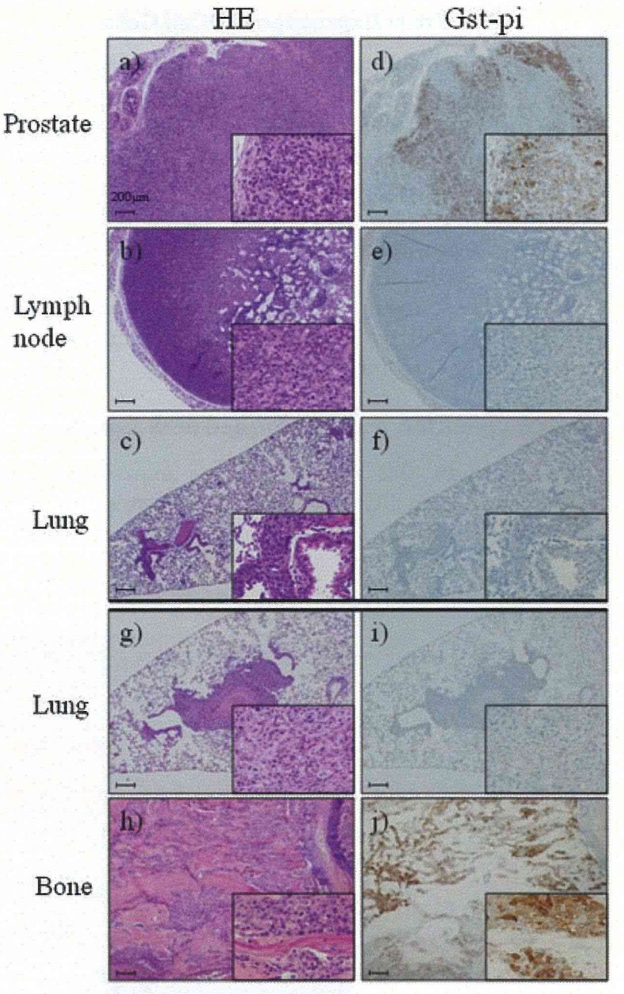

Fig. 5. Representative histopathological appearance and immunohistochemical analysis in orthotopic transplantations and tail vein injections of PCai1 cells. **a–f** show the prostate tumor and metastatic lesions 6 weeks after orthotopic transplantation of PCai1 in castrated nude mice and **g–j** show lung and bone metastatic lesions from tail vein injections of PCai1 cells 9 weeks after injection. HE staining showed that all of the tumors and metastatic lesions induced by PCai1 cells are histopathologically similar to human cases, and these lesions are compatible with poorly differentiated adenocarcinomas (a,b,c,g,h). As for the orthotopic model, the staining of Gst-pi in the prostate was higher in castrated mice (d) than in non-castrated mice (data not shown), and metastatic lesions in lymph node (e) and in lung (f) were not detected by Gst-pi staining. In contrast, Gst-pi positive staining in bone metastatic lesions was apparent (j), but in lung metastatic lesions Gst-pi positive staining was not detectable in tail vein injection models (i).

Immunohistochemical Analysis for Gst-pi in Prostate Cancer Metastatic Models

In the orthotopic in vivo model, Gst-pi showed high expression in the prostate, but no expression in

TABLE I. Frequency of Metastasis by PCai1 Cell Line

Transplantation	Castration	Sacrifice (weeks)	No. of mice	Primary tumor (%)	Metastasis (%)		
					Lymph node	Lung	Bone
Subcutaneous	−	10	4	100	−	−	−
	+	10	4	100	−	−	−
Orthotopic (prostate)	−	2	2	100	0	0	0
		5	3	100	100	33	0
	+	2	2	50	0	0	0
		6	3	100	100	75	0
Tail vein	−	5	5	−	40	80	20
		9	5	−	80	100	40

metastatic sites of lung and lymph nodes (Fig. 5d–f). However, the tumor cells injected in the tail veins resulted in tumor masses in the bone with high Gst-pi expressions (Fig. 5j). In lung (Fig. 5i) and lymph nodes, metastatic tumors did not express Gst-pi similar to that observed for lymph nodes and lung metastatic cells in the orthotopic model. These observations suggest that Gst-pi has different expression levels according to metastatic sites.

DISCUSSION

To elucidate the mechanisms of prostate cancer progression, and metastasis, physiologically relevant models are essential for understanding the human disease. Prostate cancer in the TRAP model showed marked epithelial proliferation with formation of irregular glands and luminal bridging to give a cribriform pattern, and their nuclei demonstrated enlargement and severe atypia [8]. These lesions are compatible with what are seen in human adenocarcinomas. Because of the biological complexity, bone metastatic models for prostate cancer are limited [22]. In the bone metastatic sites in our model, osteolytic areas mixed with osteoblastic areas were recognized that are similar to human cases. Therefore, our model may contribute useful information for understanding the mechanisms of prostate cancer metastasis.

The intracellular redox state balances oxidant production and antioxidant capacity of the cells based on a variety of antioxidant enzymes such as superoxide dismutase, catalase, glutathione peroxidase, and GST-pi. The glutathione redox system acts in concert to provide a coordinated network of protection against ROS accumulation and oxidative damage [23–25]. GST-pi is directly responsible for the elimination of electrophilic oxidants [23,24] especially in cancer cells characterized by rapid proliferating activity and with massive endogenous production of ROS [17].

GST-pi was usually silenced by methylation in human prostate cancer cells. However, with the acquisition of androgen-independency, our present data suggested that prostate cancer might have protective mechanisms against ROS by GST-pi signals. In our previous data, the expression level of *Gst-pi* was higher in transplantable tumors that were androgen-independent than in those that were androgen-dependent [11]. PCai1 cells in androgen-free medium had higher protein expressions of Gst-pi than in androgen-containing medium, and PCai1 tumors had higher Gst-pi expressions in castrated mice than in control mice with subcutaneous tumors and orthotopic prostate tumors in vivo. These data suggest that Gst-pi can regulate cancer cell growth by adapting to the environment. Silencing of *Gst-pi* caused significant growth inhibition of PCai1 cells, and DCFH assay revealed that intracellular ROS was significantly elevated in *Gst-pi*-siRNA and Gst-pi inhibitor treated groups. These results suggested that Gst-pi plays an important role in cell growth against ROS in PCai1 cells.

According to previous reports [26,27], the level of Gst-pi can change in response to general cellular stress. Therefore, to establish that the high expression of Gst-pi was not a reflection of cellular stress, PCai1 transplantation was performed in castrated and normal nude mice with iRNA strategy for *Gst-pi*. As a result, tumor growth of PCai1 was significantly inhibited by silencing *Gst-pi* in castrated nude mice. Therefore, Gst-pi may be necessary in androgen-independent cell growth.

Immunohistochemical analysis revealed that Gst-pi expression in subcutaneous tumors and prostate tumors in orthotopic transplants was significantly increased by castration. On the other hand, lymph nodes and lung metastatic lesions had no expression of Gst-pi. Interestingly, Gst-pi expression of the bone metastatic lesions had higher expression levels than other lesions. These findings show that Gst-pi may be

a novel therapeutic protein that can be targeted for bone metastasis.

Our newly established prostate cancer cell line PCai1, derived from the well-characterized TRAP model, may be valuable in an animal model to study the progression and metastasis of prostate cancer, and for preclinical tests of new and innovative therapeutic agents.

In summary, using our newly established prostate cancer cell line PCai1 and the metastatic models, Gst-pi expressions were shown to have important roles in prostate cancer growth and organ specific metastasis.

ACKNOWLEDGMENTS

This work was supported in part by a Grant-Aid from the Ministry of Education, Culture, Sports Science and Technology of Japan, by a Grand-Aid for Cancer Research from the Ministry of Health, Labor and Welfare of Japan, and by a Grant-Aid for Ono Pharmaceutical Co., Ltd.

REFERENCES

1. Gronberg H. Prostate cancer epidemiology. Lancet 2003; 361(9360):859–864.
2. Huggins C. Endocrine-induced regression of cancers. Cancer Res 1967;27(11):1925–1930.
3. Petrylak DP, Tangen CM, Hussain MH, Lara PN Jr, Jones JA, Taplin ME, Burch PA, Berry D, Moinpour C, Kohli M, Benson MC, Small EJ, Raghavan D, Crawford ED. Docetaxel and estramustine compared with mitoxantrone and prednisone for advanced refractory prostate cancer. N Engl J Med 2004;351(15): 1513–1520.
4. Schurko B, Oh WK. Docetaxel chemotherapy remains the standard of care in castration-resistant prostate cancer. Nat Clin Pract Oncol 2008;5(9):506–507.
5. Oh WK, Kantoff PW. Docetaxel (Taxotere)-based chemotherapy for hormone-refractory and locally advanced prostate cancer. Semin Oncol 1999;26(5 Suppl 17):49–54.
6. Shirai T. Significance of chemoprevention for prostate cancer development: Experimental in vivo approaches to chemoprevention. Pathol Int 2008;58(1):1–16.
7. Shirai T, Takahashi S, Cui L, Futakuchi M, Kato K, Tamano S, Imaida K. Experimental prostate carcinogenesis—Rodent models. Mutat Res 2000;462(2–3):219–226.
8. Asamoto M, Hokaiwado N, Cho YM, Takahashi S, Ikeda Y, Imaida K, Shirai T. Prostate carcinomas developing in transgenic rats with SV40 T antigen expression under probasin promoter control are strictly androgen dependent. Cancer Res 2001;61(12):4693–4700.
9. Said MM, Hokaiwado N, Tang M, Ogawa K, Suzuki S, Ghanem HM, Esmat AY, Asamoto M, Refaie FM, Shirai T. Inhibition of prostate carcinogenesis in probasin/SV40 T antigen transgenic rats by leuprorelin, a luteinizing hormone-releasing hormone agonist. Cancer Sci 2006;97(6):459–467.
10. Tang M, Ogawa K, Asamoto M, Hokaiwado N, Seeni A, Suzuki S, Takahashi S, Tanaka T, Ichikawa K, Shirai T. Protective effects of citrus nobiletin and auraptene in transgenic rats developing adenocarcinoma of the prostate (TRAP) and human prostate carcinoma cells. Cancer Sci 2007;98(4):471–477.
11. Hokaiwado N, Takeshita F, Naiki-Ito A, Asamoto M, Ochiya T, Shirai T. Glutathione S-transferase Pi mediates proliferation of androgen-independent prostate cancer cells. Carcinogenesis 2008;29(6):1134–1138.
12. Nelson WG, De Marzo AM, DeWeese TL. The molecular pathogenesis of prostate cancer: Implications for prostate cancer prevention. Urology 2001;57(4 Suppl 1):39–45.
13. Pathak S, Singh R, Verschoyle RD, Greaves P, Farmer PB, Steward WP, Mellon JK, Gescher AJ, Sharma RA. Androgen manipulation alters oxidative DNA adduct levels in androgen-sensitive prostate cancer cells grown in vitro and in vivo. Cancer Lett 2008;261(1):74–83.
14. Miyake H, Hara I, Kamidono S, Eto H. Oxidative DNA damage in patients with prostate cancer and its response to treatment. J Urol 2004;171(4):1533–1536.
15. Finkel T, Holbrook NJ. Oxidants, oxidative stress and the biology of ageing. Nature 2000;408(6809):239–247.
16. Nose K. Role of reactive oxygen species in the regulation of physiological functions. Biol Pharm Bull 2000;23(8):897–903.
17. Sauer H, Wartenberg M, Hescheler J. Reactive oxygen species as intracellular messengers during cell growth and differentiation. Cell Physiol Biochem 2001;11(4):173–186.
18. Feig DI, Reid TM, Loeb LA. Reactive oxygen species in tumorigenesis. Cancer Res 1994;54(7 Suppl):1890s–1894s.
19. Dakubo GD, Parr RL, Costello LC, Franklin RB, Thayer RE. Altered metabolism and mitochondrial genome in prostate cancer. J Clin Pathol 2006;59(1):10–16.
20. Chomyn A, Attardi G. MtDNA mutations in aging and apoptosis. Biochem Biophys Res Commun 2003;304(3):519–529.
21. Ripple MO, Henry WF, Rago RP, Wilding G. Prooxidant-antioxidant shift induced by androgen treatment of human prostate carcinoma cells. J Natl Cancer Inst 1997;89(1):40–48.
22. Singh AS, Figg WD. In vivo models of prostate cancer metastasis to bone. J Urol 2005;174(3):820–826.
23. Finkel T. Oxidant signals and oxidative stress. Curr Opin Cell Biol 2003;15(2):247–254.
24. Kohen R, Nyska A. Oxidation of biological systems: Oxidative stress phenomena, antioxidants, redox reactions, and methods for their quantification. Toxicol Pathol 2002;30(6):620–650.
25. Oberley LW, Buettner GR. Role of superoxide dismutase in cancer: A review. Cancer Res 1979;39(4):1141–1149.
26. Morel F, Fardel O, Meyer DJ, Langouet S, Gilmore KS, Meunier B, Tu CP, Kensler TW, Ketterer B, Guillouzo A. Preferential increase of glutathione S-transferase class alpha transcripts in cultured human hepatocytes by phenobarbital, 3-methylcholanthrene, and dithiolethiones. Cancer Res 1993;53(2):231–234.
27. Thimmulappa RK, Mai KH, Srisuma S, Kensler TW, Yamamoto M, Biswal S. Identification of Nrf2-regulated genes induced by the chemopreventive agent sulforaphane by oligonucleotide microarray. Cancer Res 2002;62(18):5196–5203.

The Prostate 72:1559–1572 (2012)

Therapeutic Targeting of Angiotensin II Receptor Type I to Regulate Androgen Receptor in Prostate Cancer

Satoru Takahashi,[1]* Hiroji Uemura,[2] Azman Seeni,[1,3] Mingxi Tang,[1,4] Masami Komiya,[1] Ne Long,[1] Hitoshi Ishiguro,[2] Yoshinobu Kubota,[2] and Tomoyuki Shirai[1]

[1]*Department of Experimental Pathology and Tumor Biology, Nagoya City University Graduate School of Medical Sciences, Nagoya, Japan*
[2]*Department of Urology, Yokohama City University Graduate School of Medicine, Yokohama, Japan*
[3]*Advanced Medical and Dental Institute, Universiti Sains Malaysia, Pinang, Malaysia*
[4]*Department of Pathology, Luzhou Medical College, Sichuan, China*

BACKGROUND. With the limited strategies for curative treatment of castration-resistant prostate cancer (CRPC), public interest has focused on the potential prevention of prostate cancer. Recent studies have demonstrated that an angiotensin II receptor blocker (ARB) has the potential to decrease serum prostate-specific antigen (PSA) level and improve performance status in CRPC patients. These facts prompted us to investigate the direct effects of ARBs on prostate cancer growth and progression.
METHODS. Transgenic rat for adenocarcinoma of prostate (TRAP) model established in our laboratory was used. TRAP rats of 3 weeks of age received ARB (telmisartan or candesartan) at the concentration of 2 or 10 mg/kg/day in drinking water for 12 weeks. In vitro analyses for cell growth, ubiquitylation or reporter gene assay were performed using LNCaP cells.
RESULTS. We found that both telmisartan and candesartan attenuated prostate carcinogenesis in TRAP rats by augmentation of apoptosis resulting from activation of caspases, inactivation of p38 MAPK and down-regulation of the androgen receptor (AR). Further, microarray analysis demonstrated up-regulation of estrogen receptor β (ERβ) by ARB treatment. In both parental and androgen-independent LNCaP cells, ARB inhibited both cell growth and AR-mediated transcriptional activity. ARB also exerted a mild additional effect on AR-mediated transcriptional activation by the ERβ up-regulation. An intervention study revealed that PSA progression was prolonged in prostate cancer patients given an ARB compared with placebo control.
CONCLUSION. These data provide a new concept that ARBs are promising potential chemopreventive and chemotherapeutic agents for prostate cancer. *Prostate 72: 1559–1572, 2012.* © 2012 Wiley Periodicals, Inc.

KEY WORDS: **angiotensin II receptor type 1; prostate cancer; androgen receptor; transgenic rat; intervention study**

Additional supporting information may be found in the online version of this article.

Grant sponsor: Ministry of Health, Labour and Welfare of Japan; Grant sponsor: Society for Promotion of Pathology of Nagoya, Japan; Grant sponsor: Ministry of Education, Culture, Science and Technology of Japan; Grant sponsor: Umehara Foundation of Yokohama Medical Group.

S. Takahashi and H. Uemura contributed equally to this work.

Conflict of Interest: None.

*Correspondence to: Dr. Satoru Takahashi, 1 Kawasumi, Mizuho-cho, Mizuho-ku, Nagoya 467-8601, Japan.
E-mail: sattak@med.nagoya-cu.ac.jp

Received 28 September 2011; Accepted 15 February 2012
DOI 10.1002/pros.22505
Published online 16 March 2012 in Wiley Online Library (wileyonlinelibrary.com).